

# Optimization of Cruciform Specimen for Low Capacity Biaxial Testing Machine

I. Guelho<sup>1</sup>, L. Reis<sup>1</sup>, M. Freitas<sup>1</sup>, B. Li<sup>1</sup>, J. F. A. Madeira<sup>2</sup>, R. A. Cláudio<sup>1,3\*</sup>

<sup>1</sup> ICEMS, Instituto Superior Técnico, UTL,

Av Rovisco Pais, 1049-001 Lisboa, Portugal

<sup>2</sup>IDMEC-IST, Instituto Superior Técnico, UTL,

Av Rovisco Pais, 1049-001 Lisboa and ISEL, Portugal

<sup>3</sup>ESTSetúbal, Instituto Politécnico de Setúbal,

Campus do IPS, Estefanilha, Setúbal, Portugal.

E-mail: [ricardo.claudio@estsetubal.ips.pt](mailto:ricardo.claudio@estsetubal.ips.pt)

**ABSTRACT.** *One of the most restricting aspects of the biaxial fatigue test is the design of the cruciform specimen. Nowadays, with the introduction of the new in-plane biaxial fatigue testing machines, based on linear electrical motors, with much lower force capacity than conventional hydraulic machines, make the optimization of the cruciform geometry crucial for successful biaxial tests. The aim of this paper is to investigate the influence of the geometric design on the stress distribution in cruciform specimens and optimize the shape of the cruciform specimens under biaxial loading conditions. The optimization is performed with two main objectives: to concentrate and initiate fatigue damage in the center of the specimen within a uniform stress region, and to minimize undesirable phenomena, such as premature failure outside the area of interest due to stress concentrations. For treating with the multi-objective optimization problem (MOO) presented, a new derivative-free methodology, called direct multi-search (DMS) method is used in order to determine the non-dominated points of the Pareto front. The evaluation is made with finite element analysis (FEA) software, ABAQUS, which uses PYTHON language for scripting. The optimization processes give much improved results and are validated by experiments.*

## INTRODUCTION

Biaxial testing is required to study the deformation and fatigue behaviour of a particular material. The most common method of biaxial testing employs thin-walled cylinder tubes subjected to axial and/or torsional loads and internal pressure. The disadvantages of this method are that it has limited loading capacity for simulating the biaxial tension/tension loading conditions and it requires the material to be in the form of a circular tube, so it cannot be applied to rolled sheet materials and some composite material. Therefore, there has been a steadily-growing interest in biaxial testing of cruciform geometries (i.e., two-dimensional analogues of the uniaxial tensile geometry).

A variety of geometric features have been developed all over the years for cruciform specimen design. The first geometry shown in Figure 1, where very thin slits are cut into the arms, was proposed by Kuwabara et al. [1] and reports that the slits promote uniform strains within the inner part of the gauge area, irrespective of the loading ratio. A second feature is a smooth notch geometry added to the four corners of the gauge area [2], as shown in Figure 2. The intention is to promote higher strains in the gauge area. A third feature is a reduction in thickness within the gauge area to further localize deformation there [3]. An example is shown in Figure 3, which contains a central “recessed” region (denoted by the solid circle in the gauge area). Combinations of the aforementioned features have been proposed in Green et al. [4], examples of these are shown in Figure 4.

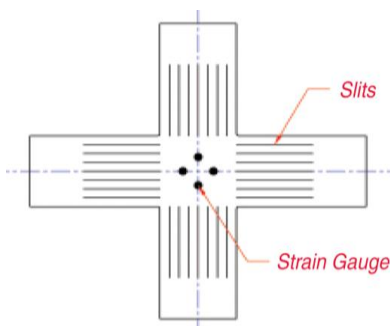


Figure 1 – Very thin slits cut in the spokes.

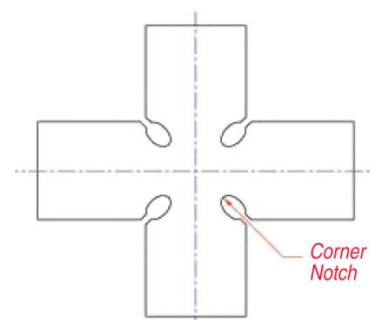


Figure 2 – Smooth corner notch added between the arms.

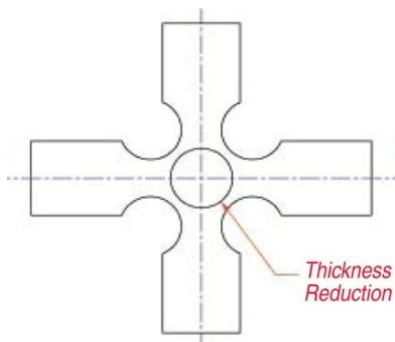


Figure 3 – Reduction in thickness within the gauge area.

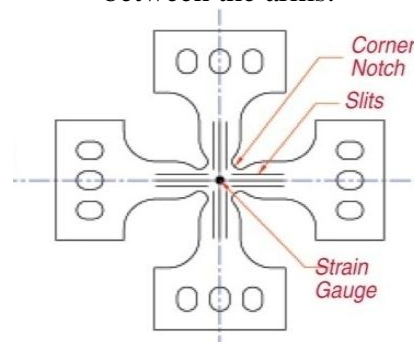


Figure 4 – Combinations of the aforementioned three features.

In reference [5], the influence of geometrical discontinuities on the strain distribution in biaxial loaded specimens was studied in detail. A numerical optimization methodology was proposed by Makris [6] to achieve higher quality biaxial tests by modifying the specimen’s geometry.

In the present paper, the cruciform specimen studied is being tested in a new biaxial fatigue testing machine based on a recent technology of linear electrical motors. The machine uses four of the most powerful iron core linear motors available in the market for industrial applications, and with a new guiding system based on air bearings which provide very high precision movement without contact. However, its maximum loading

capacity is about 4 kN in each direction [7], which is much lower than conventional hydraulic machines. Therefore, it is particularly important to optimize the shape of the cruciform specimen in order to achieve fatigue crack initiation in the central gauge area with such low force involved.

Direct multi-search (DMS) method is used to obtain the Pareto front relating the two objectives functions: (i) maximize stress at the gauge area and (ii) minimize stress in the arms/corner. The evaluation of the objective functions was made with the commercial software ABAQUS for finite element modeling and solver. The PYTHON language is used as interface between MATLAB and ABAQUS programs for scripting all the input geometries specimen design.

## CRUCIFORM SPECIMEN DESIGN

After reviewing numerous cruciform geometries presented in the literature, the specimen geometry presented here derives from cruciform geometry with reduced thickness at center, Fig. 3. Considering the two main objectives, the first focus goes to the minimization of stress concentration in the arms corners from chamfers to circular fillets, convex fillets, elliptical fillets, etc., as presented by Abdelhay et al., [8]. The second objective is to achieve the maximum stress at the center gauge area in a uniform stress region where the fatigue crack initiation should start. The best geometry is found to be the elliptic fillet as shown in Fig. 5, which better allocates stresses at the center without increasing into the corners. The design variables for the optimization process, initial values of each variable and limits are presented in table 1.

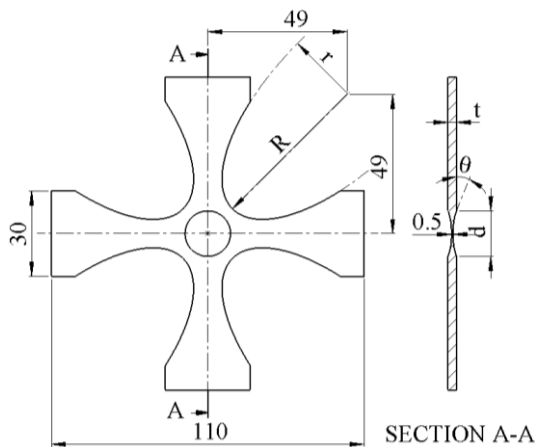


Figure 5 – Specimen geometry.

Table 1 – Design variables.

Variable	Init.	Min.	Max.
Arm thickness, $t$	4	3	5
Minor Ellipse Radius, $r$	24	22	26
Major Ellipse Radius, $R$	57.5	56	59
Centre spline diameter, $d$	17	14	20
Spline exit angle, $\theta$	60	30	90

Dimensions in [mm] or [°]

In this specimen the thickness at center was fixed as 0.5 mm, stipulated as being the minimum value to ensure good machining conditions, [9]. The center geometry is created by a revolving spline with a tangency of  $0^\circ$  at center and exiting with an angle  $\theta$  at a diameter  $d$ . This spline ensures a smooth geometrical transition to avoid stress concentration in the critical region.

## MULTI-OBJECTIVE OPTIMIZATION

A constrained nonlinear MOO can be mathematically formulated as, [10]:

$$\text{find } X = \{x_1, x_2, \dots, x_n\}^T \quad (1)$$

which minimizes:

$$\min F(x) \equiv \{f_1(x), f_2(x), \dots, f_k(x)\}^T \quad (2)$$

subject to:

$$\begin{aligned} g_{l_1}(x) &\leq 0, & l_1 &= \{1, 2, \dots, m_1\} \\ h_{l_2}(x) &\leq 0, & l_2 &= \{1, 2, \dots, m_2\} \end{aligned} \quad (3)$$

where  $x$  are the design variables,  $n$  is the number of design variables,  $f$  are the objective functions,  $k$  is the number of objective functions to be minimized and  $m_1$  and  $m_2$  are the number of constraint equations. Any or all functions  $f_i(x)$ ,  $g_{l_1}(x)$  and  $h_{l_2}(x)$  can hold a nonlinear nature. In general, since in MOO there are often conflicting objectives for each objective function, the concept of Pareto dominance is used to characterize global and local optimality, [10]. A feasible solution of  $X$  is called a Pareto optimal if there exists no other feasible solution  $Y$  such that  $f_i(Y) \leq f_i(X)$  for all  $i = \{1, 2, \dots, k\}$  with  $f_j(Y) < f_j(X)$  for at least one  $j$ ,  $j \in \{1, 2, \dots, k\}$ .

DMS is a solver for multiobjective optimization problems, without the use of derivatives and does not aggregate any components of the objective function. It essentially generalizes all direct-search methods of directional type from single to multiobjective optimization, maintaining a list of feasible nondominated points. At each iteration, the new feasible evaluated points are added to this list and the dominated ones are removed. Successful iterations correspond then to an iterate list changes, meaning that a new feasible nondominated point was found. Otherwise, the iteration is declared as unsuccessful.

## OPTIMIZATION PROCEDURE

As represented in Fig. 6 the optimization starts by establishing the new geometry variables (input variables) of the new specimen in MATLAB, regarding all the geometrical and objective constrains. Then, these variables are exported to an input file which is read by the PYTHON script. Afterwards, the finite element model based on the geometry is generated and the ABAQUS "Job" input file created. The ABAQUS is then used as a "solver" in order to determine all the stresses in the regions of interest by the Von Mises criterion. The design variables are the arm thickness ( $t$ ), minor ellipse radius ( $r$ ), major ellipse radius ( $R$ ), centre spline diameter ( $d$ ) and the spline exit angle ( $\theta$ ), whose initial values and limits (introduced as restrictions) are given in Fig. 5. Another restriction was introduced, limiting the maximum difference of stress on a circular area with a diameter of 4 mm below 5%, to ensure that the stress at the centre of the

specimen is uniform. The objective functions are the  $f_1$  the stress at centre (in this case the value of stress is multiplied by -1 to solve a minimization problem) and  $f_2$  the maximum stress in the arm curvature.

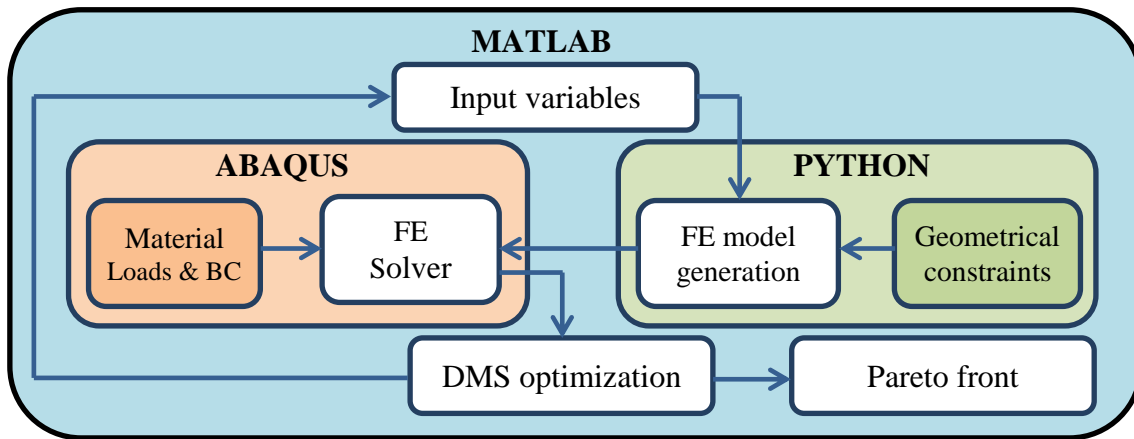


Figure 6 – The integration software framework.

The finite element model represents 1/8 of the whole specimen, being applied appropriate symmetry boundary conditions. A distributed load of 3 kN was applied in each arm, which is about 75% of the maximum force available in our test machine. Discretization was made with 27315 hexahedral elements with 20-nodes and full integration (C3D20 in ABAQUS code), being obtained a regular mesh with 15  $\mu\text{m}$  edge size elements at centre. The material considered is an aluminium alloy with Young modulus of 210 GPa and Poisson ratio of 0.3.

## OPTIMIZATION RESULTS

Table 2 presents the results of several simulations (these are not the optimum results, neither represent the pareto front) in order to evaluate the effect of each variable in the centre area stress and in the arms. Darker cell identify the parameters that were changed relative to a reference geometry with  $t = 4,0$  mm;  $r = 24$  mm;  $R = 59$  mm;  $d = 18$  mm and  $\theta = 30^\circ$ . The optimum values, which verify all the restrictions, are presented in the last line in bold.

### *Arms thickness influence, $t$*

The ratio between the thickness at the arms and the center cannot also be disregarded. In fact, they are responsible for the global stiffness of the specimen and consequently the stresses accomplished in all partitions. In this work, the thickness considered at the center is fixed as 0.5 mm, which is the minimum value that guarantees good machining quality, [8].

Table 2 – Influence of design variables on final results.

t [mm]	r [mm]	R [mm]	d [mm]	$\theta$ [°]	Center area Stress ( $-f_1$ ) [MPa]	Arms Stress ( $f_2$ ) [MPa]	Diff. at center [%]	Corner/ center diff. [%]
3,0	24	59	18	30	177,5	150,2	1,854	15,354
4,0	24	59	18	30	152,7	108,4	6,589	29,015
5,0	24	59	18	30	134,9	83,4	13,452	38,175
4,0	22	59	18	30	153,0	113,9	6,583	25,578
4,0	23	59	18	30	152,8	110,9	6,586	27,371
4,0	24	59	18	30	152,7	108,4	6,589	29,015
4,0	25	59	18	30	152,5	109,3	6,591	28,344
4,0	26	59	18	30	152,4	117,5	6,596	22,906
4,0	24	57	18	30	119,1	81,2	6,569	31,834
4,0	24	58	18	30	133,6	92,1	6,579	31,046
4,0	24	59	14	30	138,7	102,8	16,415	25,861
4,0	24	59	16	30	144,4	102,6	10,197	28,924
4,0	24	59	18	45	156,3	125,3	2,406	19,832
4,0	24	59	18	60	159,9	147,1	1,286	8,015
4,0	24	59	18	75	163,6	171,4	0,904	-4,753
<b>3,0</b>	<b>22</b>	<b>59</b>	<b>15</b>	<b>30</b>	<b>160.3</b>	<b>130.1</b>	<b>3,705</b>	<b>20,327</b>

### *Elliptical fillet influence*

The elliptic fillet proposed for the arms corner is managed essentially by two parameters, the major and the minor radii. The results from the FEA show that the increase of the ellipse major radius also increases stress in the central gauge area, however, the inherent stiffness decrease due to the material loss in the corner creates stress concentration. On the other hand, the minor radius of the ellipse is directly related with the stress distribution in the arms and will also determine a smooth or rough transition in the same corner.

### *Centre spline diameter, d*

The center spline diameter defines the diameter of the region with reduced thickness that is created with a spline. This parameter has a strong influence in the stress uniformity at center and some influence in the maximum stress at center. If  $d$  increases the uniformity of stress decreases but the maximum stress value increases.

### *Spline angle effect, $\theta$*

The introduction of a spline in the central gauge area, where the thickness reduction occurs, turns out to be one of the best ways to avoid stress concentrations and to control the amount of stresses transmitted to the corner from the central region. A large stress concentration is created in the arms if  $\theta$  increases without a significant increase of stress in the central region.

### Optimized geometry

The results obtained from the DMS optimization are expressed in the follow Pareto front distribution, see fig. 7, where the optimum value chosen from the non-dominated points, contemplates two constrains: maximum stress in the center gauge area ( $f_1$ ) assuring a safety factor of 20% between the arms ( $f_2$ ) and the center gauge area stress; uniform stress in the central region with less than 5% of difference in a 4 mm diameter. This safety factor was stabilized according to our experience in experimental tests. If the stress in the arms are below 20% is enough to guarantee that failure will not occur in the arms. The geometry and FEM solution corresponding to the optimum point is represented in Fig. 8 for 1/8 of the cruciform geometry. This solution is for the parameters given in last line of Table 2.

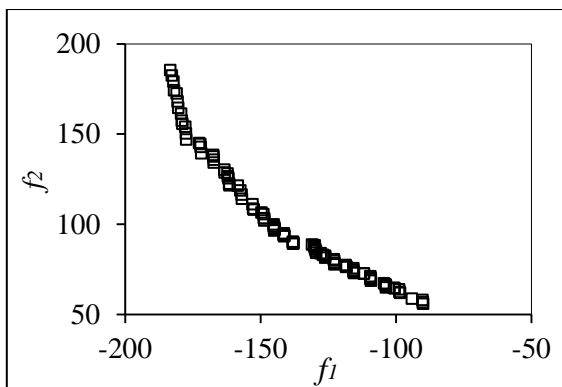


Figure 7 – DMS - Pareto Front.

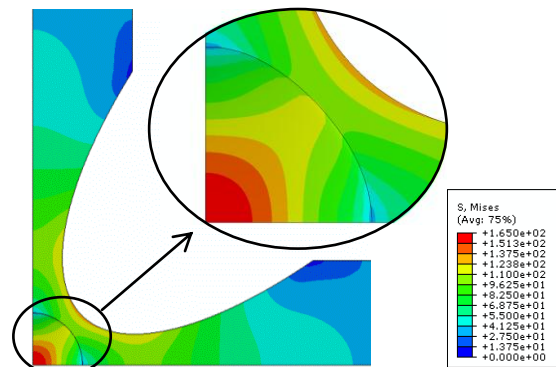


Figure 8 – Stress distribution in the optimized cruciform geometry.

Experimental validation of the optimized geometry has also been carried out. Several specimens, with a geometry close to the optimized, were successfully tested with the aforementioned biaxial fatigue machine, [9], demonstrating that this geometry is appropriated for fatigue crack initiation.

## CONCLUSIONS

The influence of several design variables on centre area stress and in the arms was studied for a biaxial specimen appropriate for fatigue crack initiation. In general if the design variables are changed in such way that the stress in the centre increases, also the stress uniformity decreases and larger stress are created in undesirable regions like for example in the arms.

Geometry optimization based on FEA programing coupled with direct multi-search method is an efficient way to determine the best combination of the design variables ensuring a high level and uniform stress in the centre of the specimen without creating excessive stress in other region that could cause failure outside of the gauge area.

The results obtained from the Pareto front show that there are several optimum geometries. From the Pareto front, the designer can pick one of the optimal solutions (non-dominated solutions), depending on the relative importance of each objective. The results also illustrate the capacity of this DMS model to solve the optimization problem in a reasonable amount of time.

Several specimens were machined and fatigue tests were conducted for crack initiation in a low capacity biaxial test machine. It was observed that failure occurs in the central region and very good experimental validation was shown.

## ACKNOWLEDGEMENTS

The project is supported by FCT project ref. PTDC/EME-PME/102860/2008, "Deformation and fatigue life evaluation by a new biaxial testing system".

## REFERENCES

1. Kuwabara, T., Ikeda, S. and Kuroda, K., (1998) *J. of Mat. Proc. Tech*, **80–81**, pp.517–523.
2. Müller, W. and Pöhlandt, K., (1996) *J. Mat. Proc. Tech.*, **60**, pp.643–648.
3. Ghiotti, A., Bruschi, S., and Bariani, P., (2007) *Key Eng. Mat.*, **344**, pp.97–104.
4. Green, D., (2004), *Int. J. of Plasticity*, **20**, pp.1677–1706.
5. Lamkanfi, E., Van Paepegem, W., Degrieck, J., Ramault, C., Makris, A., and Van Hemelrijck, D. (2010), *Polymer Testing*, **29**, pp.132–138.
6. Makris, A., Vandenbergh, T., Ramault, C., Van Hemelrijck, D., Lamkanfi, E., and Van Paepegem, W., (2010), *Polymer Testing*, **29**, pp.216–223.
7. Freitas, M., Reis, L., Li, B., Guelho, I., Cláudio, R.A., Antunes, V. and Maia, J., (2013) In-plane biaxial fatigue testing machine powered by linear iron core motors, *Sixth Symp. on Application of Automation Tech. in Fatigue and Fracture Testing and Analysis*, **ASTM STP 1571**.
8. Abdelhay, A.M., Dawood, O. M., Bassuni, A., Elhalawany, E. A. and Mustafa, M.A. (2009) "A Newly Developed Cruciform Specimens Geometry for Biaxial Stress Evaluation Using NDE", *Int. Conf. on Aerospace Sciences & Aviation Tech*, **ASAT-13-TE-12**.
9. Cláudio, R.A., Freitas, M., Reis, L., Li, B. and Guelho, I. (2013) "Multiaxial Fatigue Behaviour of 1050 H14 Aluminium Alloy by a Biaxial Cruciform Specimen Testing Method", *10th Int. Conf. on Multiaxial Fatigue and Fracture*.
10. Custódio, A.L., Madeira, J.F.A., Vaz, A.I.F. and Vicente, L.N., (2011) *SIAM Journal on Optimization*, **21**, pp.1109-1140.